Sharpening our thinking about polar cap ionospheric patch morphology, research, and mitigation techniques

Herbert C. Carlson[1]

Received 29 November 2011; revised 6 April 2012; accepted 12 April 2012; published 31 May 2012.

[1] Since polar cap patches were discovered, their nature, physics, and impact on navigation and communication signals has been repeatedly addressed. Both terminology and inference of physical processes from diverse instruments have introduced confusion. Poleward moving auroral form is a morphological descriptor but cannot be equated to an island of high-density plasma. Particle precipitation produces low-density patches, but high-density patches derive from solar produced plasma. The challenge of patches is finding the dominant mechanism for chopping entering ionization into islands (∼100–1000 km in size). Velocity-dependent recombination physics is valid in principle but not relevant to patches formed in at least the European sector. Most patches are formed by transient magnetic reconnection events. While the plasma is at too high an altitude for the strong velocity shears to erode plasma densities, the shears become the dominant plasma structuring mechanism until the initial magnetic tension force is relaxed. Initial patch structuring is not by gradient drift as believed for decades but rather by the shear driven instability, impacting mitigation techniques. Large-scale shears, driven to 2–3 km/s, impact satellite drag through thermospheric heating. The study here is intended to sharpen understanding of patches for future research and development of techniques for mitigation of their effects on navigation and other systems dependent on receiving radio frequency signals from satellites and understanding reconnection driven impact on thermospheric density and satellite drag.

Citation: Carlson, H. C. (2012), Sharpening our thinking about polar cap ionospheric patch morphology, research, and mitigation techniques, *Radio Sci.*, *47*, RS0L21, doi:10.1029/2011RS004946.

1. Introduction

[2] Over the past half dozen years knowledge has advanced significantly regarding the physics on which to base solutions to outages of high-latitude/polar communications and GPS/GNSS signals, and anticipate boundaries for radar clutter, HF signal disruption, and blurring of satellite radar imaging. This allows planning to move from climatology or time-dependent climatology, to physics based now and forecast.

[3] We have known for decades that polar cap "patches" (∼100–1000 km islands of plasma at least double the density of surrounding background plasma) of high-density solar-EUV-produced ionospheric plasma can enter the polar cap through the cusp dayside auroral region, transit the polar cap at ∼km/s speeds, and exit the polar cap hours later near midnight to enter return sunward flow patterns. This can impact radio frequency (RF) systems because the patches becomes structured to scale sizes ∼100s km to ∼10 m, thus affecting RF systems at HF-GHz frequencies. Below 10 km scales structuring [*Basu et al.*, 1990] by the gradient drift instability structuring migrates into the body of the patch from the trailing edge of the patch, that by the shear driven instability [*Basu et al.*, 1988b] from the side along the shear line. *Tsunoda* [1988] reviewed high-latitude F region irregularities, *Weber et al.* [1986] analyzed a transpolar event. When the patches are as dense as 10^6 cm^{-3}, or equivalently expressed as foF2 [the maximum ordinary mode radio wave frequency capable of reflection from the F2 region of the ionosphere] ∼9 MHz they cause [*Weber and Buchau*, 1981; *Basu et al.*, 1987, 1988a] severe communication/navigation outages when they intersect the RF line of sight between the receiver to the satellite RF source. For foF2s much lower, scintillation effects are less. We seek to summarize here several recent mutually connected discoveries, listed in section 8, that explain previously unanswered key questions, and correct some misperceptions that previously persisted for decades.

[4] Before getting into recent advances however, let us offer a broader picture of understanding of polar cap patches, with emphasis on past and recent model polar ionospheric "patch" studies. Done without the extensiveness of a full review, this will serve as context for the following specific focus on both most recent advances in understanding, and on the logic path of linkages among these advances, emphasizing reconnection transients.

[1]Space Weather Center, CASS, Utah State University, Logan, Utah, USA.

Corresponding author: H. C. Carlson, Space Weather Center, CASS, Utah State University, Logan, UT 84322, USA. (herbert.c.carlson@googlemail.com)

0048-6604/12/2011RS004946

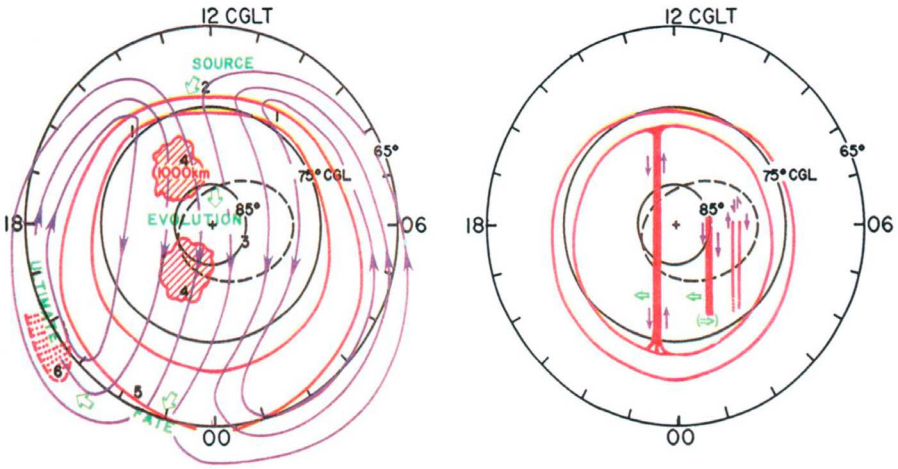

Figure 1. View in Earth-Sun frame of reference of conditions characterizing the state of the polar cap ionosphere for southward and northward IMF and positive *By*. For negative *By* the patterns are mirror imaged about a noon-midnight axis of symmetry. A nominal auroral oval location is shown for each condition, on CGLT coordinates from 65° magnetic latitude, looking down on the north magnetic pole. Convection is shown by closed flow lines with arrows overlaid (southward IMF) or thin adjoining arrows (northward IMF). Cross-hatched areas show recombination 630.0 nm enhancements from high plasma density patches (southward IMF); Sun-aligned bars show electron impact 630.0 nm enhancements (northward IMF). Open arrows show the direction of motion of these polar 630.0 nm features. The dashed line ellipse near the central polar cap is the field of view of an all-sky imaging photometer (ASIP) at the latitude of Thule, for 250 km emissions. Note that for this CGLT coordinate system, fixed magnetic latitudes are circles, so circular fields of view appear as ellipses [*Carlson*, 1994]. All these descriptions are for dark Northern Hemisphere polar cap winter conditions. The same physical phenomena must occur in the summer sunlit pole, but the degree of change in ionospheric properties and signatures will be largely masked and/or subdued by the ionospheric plasma locally produced by the sunlight (EUV for the *F* region ionosphere). Plasma transported from large distances dominates the character of the winter conditions, whereas locally produced plasma dominates the summer conditions. The polar ionosphere for southward versus northward IMF is characterized by quite different properties of the overhead sky seen by an ASIP, a digital ionosonde (Digisonde), or a total electron content (TEC) polarimeter receiver of signals from a satellite radio beacon. Thus, such ground-based measurements can serve as surrogate indicators of the north-south sense of the IMF (from *Carlson* [1994]).

1.1. Background

[5] A special section of *Radio Science* in 1994 was a milestone capturing progress on understanding the polar cap ionosphere up to 1994. In the introduction to that special section, *Carlson* [1994, Figure 1] distinguished the northward from the southward IMF state of the polar cap ionosphere, and offered a framework for future progress on key Southward IMF polar cap patch issues, of what controls their: source, transpolar evolution, exit, and ultimate return flow fate. That is reproduced as Figure 1 here, to track progress made and yet to be made. Significant progress has been made on understanding the entry, transpolar evolution, and locations of exit. The specific mechanism(s) for exit, and much about the ultimate fate of the return flow "blobs" has yet to be laid to rest. Future focus is moving to coupling of forcing by and energy from the Solar Wind, and via the magnetosphere, and consequences to the thermosphere. Several full reviews of knowledge of polar cap patches and polar cap Sun-aligned arcs have appeared since 1994. Space Weather issues in general are discussed by *Schunk and Sojka* [1996]. *Crowley* [1996] did a critical review of patches and blobs. For polar cap patches and arcs, see special section on CEDAR HLPS/STEP GAPS in *Radio Science, 31*, 573–678, 1996, and *Basu and Valladares* [1999]. The northward IMF (Interplanetary Magnetic Field) polar cap state, characterized by Sun-aligned arcs, has been reviewed by *Smith and Lockwood* [1996], *Zhu et al.* [1997], and *Sandholt et al.* [2002].

[6] Technological impact of the science applies to the RF spectrum from HF communication/sensing, through satellite UHF communication, up through GPS navigation frequencies. *Basu et al.* [1988a] starkly quantified the degree of degradation of radio frequency signals from satellites. Based on 8 years of polar cap scintillation data from Thule, Greenland, monitoring 244 MH signals from a USAF polar beacon satellite (at high elevation angles which do not accentuate ionospheric scintillation effects), they documented that 15 min fade depths exceed 10 db over 50% of the time for each of the five winters sampled during the sunspot maximum years 1979–1982, and 20 db at least 10% of the time in these midwinters, but are present less than 5% of the time for sunspot minimum years 1985–1986.

1.2. Two Characteristic Polar Cap States

[7] The polar ionosphere and upper atmosphere alternate between two states, depending on whether the IMF is

southward or northward. This is indicated in Figure 1. This alternation is due to the very different degree of coupling between the solar wind and the magnetosphere, for opposite signs of the north-south (z) component of the IMF *Bz.* For southward IMF, called negative *Bz*, the coupling is very strong, and such strong coupling can have severe effects on radio signals. Ground-based optical and radio measurements in the polar cap respond in a way so reliably and so strongly coupled that their measurement can show in real time which of these two states prevails. This correlation was established through the use of satellites measuring the full IMF vector (and solar wind speed, density and temperature). Satellites "parked" at the location where the Earth's and Sun's gravitational fields balance are upstream of Earth in the solar wind, and can therefore give us early warning of IMF changes about an hour before corresponding conditions switch at Earth. The transverse east-west *By* components of the IMF introduces an east-west or dawn-dusk asymmetry, the effects of the *Bx* component which is along the Sun-Earth line are more subtle. IMF changes can occur over scales of minutes or less distinguishing the polar cap ionosphere from the rest of the globe, with which it shares other strong dependencies on the solar cycle, and seasonal and diurnal variations (recall the polar day/night in summer/winter is months long).

[8] Strong scintillation is associated with southward IMF, while northward IMF leads to much weaker scintillation. This is because southward IMF can produce ionospheric patches, while northward IMF does not. We thus turn focus now to southward IMF conditions and polar cap ionospheric patches, of practical concern for mitigation/circumvention of consequences to satellite communication, GPS navigation, satellite radar imagery, and HF communication and sensing.

1.3. Southward IMF State

[9] The state for southward IMF is characterized in midwinter by ~100–1000 km islands, or patches, of enhanced *F* region plasma, surrounded by lower-density plasma. As these patches pass overhead, the overhead ionosphere can switch sharply between peak plasma densities $\sim 10^5$ cm^{-3}, and $\sim 10^6$ cm^{-3} [*Weber et al.*, 1984], values which respectively correspond to an ionospheric foF2 of 3, and 9 MHz in the HF band. This excursion is literally from night to day (from typical electron densities found near midnight to near midday at midlatitudes). The term "patches" derives from their patchy appearance in 630.0 nm imagers, which discovered them [*Weber and Buchau*, 1981]. By convention [*Crowley*, 1996], high electron density islands, double or more their surrounding densities, are termed patches. Patches move antisunward across the polar cap, at ~1 km/s from near noon toward midnight. A patch formed over Svalbard, Norway, passes over Alaska about an hour or two later. Its transpolar trajectory is taken to be consistent with a normal two-cell convection pattern [*Heelis*, 1984] defined by averaged flow patterns of ionospheric plasma in the polar cap for southward IMF.

1.4. Patch Theory and Modeling

[10] To model patch behavior, one needs to be concerned with the source reservoir of plasma for patches; a mechanism for patch creation; the transpolar trajectory of patch path after entry into polar cap; the structuring of patch from creation to exit; the exit process for the patch; and its return sunward flow, with the possibility of recycling.

[11] First though, geomagnetic versus geographic coordinates are essential to patch morphology. The frequency of patch occurrence in the polar cap has been studied from ground stations measuring *F* region peak electron density and total electron content, and by satellites passing through the topside F region. *Rodger et al.* [1994] give a good summary of the characteristics of patches. Many ground based statistics have been published [e.g., *McEwen and Harris*, 1996; *Dandekar and Bullett*, 1999]. A comprehensive study by *Coley and Heelis* [1998], using DE in situ satellite (at about 840 km) above 75° magnetic latitude and for southward IMF, found the occurrence frequency peaks during winter during ~12 to 24 UT. Patch occurrence is suppressed in summer because the daytime sunlit polar cap electron densities are already large, and difficult to double by transporting plasma from elsewhere. The UT dependence is due to the magnetic pole displacement (about 10° in the Northern Hemisphere) from the Earth's axis of rotation. The magnetic pole (and cusp entry region) dip 10° more deeply into lower-latitude sunlit plasma in the Canadian sector, and 10° farther from sunlit plasma across Siberia. Thus for favored UTs the magnetic entry region tips more deeply into lower-latitude sunlit high-density plasma; for unfavored UTs it draws from dark low-density plasma. This difference largely explains the Northern Hemisphere UT dependence of patch occurrence. As the magnetic pole offset is not symmetric north to south pole, neither is the patch frequency of occurrence. As the auroral oval expands (or contracts) sunlit plasma will be drawn upon for a longer (or shorter) fraction of the day, giving day to day differences.

1.5. Plasma Source

[12] Solar EUV-produced plasma density in this subauroral reservoir has well-documented seasonal and solar cycle variations, which reflect in variations in peak densities drawn into the polar cap. At times, events significantly enhance the plasma densities in the reservoir, and in its path between its region of solar EUV production and the cusp. These events can have very dramatic temporal/longitudinal consequences for the reservoir [*Foster et al.*, 2005] that trace all the way across the polar cap. In the last decade or so, major progress has been made in understanding such processes, in the observing networks to track them, and in modeling them. Afternoon to premidnight electron densities at the equatorward edge of the trough can become significantly enhanced early in magnetic storms, a phenomena referred to as storm enhanced density (SED) [*Foster*, 1993]. This enhanced plasma is then transported toward noon by electric fields referred to as subauroral polarization streams (SAPS). This westward flowing plasma, which can have major density increase through downward drainage of plasmaspheric plasma into the ionosphere, is not only of major interest to global ionospheric behavior, but can dramatically increase patch densities [*Foster et al.*, 2005].

[13] Particle precipitation in the cusp [*Rodger et al.*, 1994] is no doubt also a source of patch plasma. While an important patch source, modeling indicates this source cannot explain the intense [9 MHz foF2] patches that lead to the most intense scintillation. *Oksavik et al.* [2006] have shown

particle precipitation within the polar cap can also produce patches, these too are relatively weak.

[14] We distinguish here between the plasma reservoir, and the mechanism that draws upon this reservoir to form patches by pulling them into the polar cap in segmented islands. When the magnetic pole tips toward the Sun, so the magnetic cusp entry region continuously taps high-density plasma, one does not get a continuous smooth tongue of high-density plasma crossing the polar cap. To the contrary, the plasma is segmented, and the segments are severely structured, where the segmentation process is likely critical to the structuring. What leads to this segmentation?

1.6. Patch Production Mechanisms

[15] While there are many ways in which polar cap patches can be formed, and at least six mechanisms have been published, there has in the past been no agreement as to which one(s) are most important or dominate [*Anderson et al.*, 1988; *Lockwood and Carlson*, 1992; *Sojka et al.*, 1993; *Rodger et al.*, 1994; *Valladares et al.*, 1994, 1998; *Prikryl et al.*, 1999]. *Sojka et al.* [1994] have modeled their UT and seasonal dependence.

[16] Mechanisms proposed include: discrete changes in IMF *By*, *Bz*, and solar wind density, speed and pressure; time variation of average flow pattern models [e.g., *Anderson et al.*, 1988]; plasma flow jet channels in which relative velocity–dependent recombination rates cut continuous tongues of plasma into segments [*Valladares et al.*, 1998]; IMF reversals and plasma production by cusp particle precipitation [*Rodger et al.*, 1994; *Millward et al.*, 1999]; and transient magnetopause reconnection [*Lockwood and Carlson*, 1992]; followed by Alfven wave coupling [*Prikryl et al.*, 1999] of the solar wind to the ionosphere. *Anderson et al.* [1988] and *Sojka et al.* [1993] have modeled patch production by time varying convection, and *Anderson et al.* [1996] have modeled boundary "blobs" using time varying convection. The problem is not how patches might be produced, because a discrete change in many parameters can do that. The real question needs to be, how are most observed patches produced?

[17] *Rodger et al.* [1994] associated patch formation with a precursor strong plasma azimuthal flow change, proposing variations in IMF *By* as the segmentation process, and gave evidence supporting his call for modeling of precipitation as a patch plasma source. Subsequent modeling showed cusp particle precipitation can produce patches up to ~5 MHz foF2. Many observations have come to support associating patch production with high-velocity plasma flow sheers. Models show cusp precipitation can produce patches of ~5 MHz, but cannot explain the common 9 MHz patches, which produce severe scintillation of most concern.

[18] The increased recombination in high-speed flow channels can, in principle, segment continuous tongues of high-density plasma entering the polar cap, to produce patches [*Valladares et al.*, 1994, 1998]. With adequate resolution of high-speed plasma flow channels this can be experimentally tested. *Moen et al.* [2006] have observed entering patches that appear presegmented at order one to a few 100 km scale size, and have suggested penetration electric fields as the explanation. Using time varying convection *Anderson et al.* [1988] have modeled patches by switching between different average large-scale flow patterns does lead to patch-like structures; most patches observed to enter through the cusp appear however to enter by discrete transient events.

[19] Finding the dominant patch production mechanism, though challenging, is of more than academic interest. The production mechanism defines signatures for early identification, early tracking of direction, and even where in the polar cap scintillation producing irregularities set in [*Moen et al.*, 2000].

[20] Recently the transient magnetopause reconnection mechanism for creating patches, has been put to a definitive test [*Carlson et al.*, 2002, 2004, 2006] discussed in detail in the next section. *Carlson et al.* [2006], using the Svalbard EISCAT Radar (ESR) with supporting ASIP (all sky imaging photometer) data, showed detailed agreement between model prediction and observations during an extended series of patches, observed entering the polar cap from an initially corotating subauroral plasma reservoir. The mechanism is a transient poleward excursion of the boundary separating corotating from poleward moving plasma. The boundary then relaxes poleward. Details to support the case for such observations establishing this as the dominant mechanism producing patches in at least the European sector are given in the next section.

[21] Now we move from background, to recent insights associated with a magnetic reconnection view of the cusp.

2. Patch Formation/Injection

[22] Recall, solar EUV production can provide the reservoir of high-density plasma (up to equivalent to a 9 MHz foF2), and when magnetic and geographic cusp latitude alignment favors entry of sunlit plasma through the cusp, plasma flow through the cusp can transport a tongue of higher-density plasma into the lower plasma density polar cap. Particle precipitation can also provide a reservoir of moderate density plasma (up to equivalent to a 5 MHz foF2). This however still requires a mechanism to segment any of this ionization that might enter the polar cap (upon entering, this plasma contrasts with other plasma densities dependent on flow variably reaching back to other plasma reservoirs of different higher densities [*Anderson et al.*, 1988]).

[23] Not until an incoherent scatter radar (ISR) measurement capability was created [*Carlson et al.*, 2002] to measure the four basic plasma properties electron density (Ne) and temperature (Te), ion temperature (Ti) and velocity (Vi) over an area ~600 km by ~1000 km, with ~2 min time resolution, was it possible to put the various mechanisms proposed for creating patches to definitive test.

[24] Figure 2 (left) maps a high-density Ne patch (red) coincident in time/space with a narrow channel of high-speed velocity (Figure 2, right) plasma flow (blue) measured with the required time/space coverage/resolution. A narrow high-speed flow channel could segment a high-density tongue of plasma by rapid (temperature or velocity dependent) recombination of plasma within the high-speed channel, leading to low-density plasma in the channel relative to the background higher density of the tongue. However, what we see here is the opposite, the density is high in the flow channel, not low. Thus this mechanism has the wrong sign [*Carlson et al.*, 2002] for this explanation, at least in the European sector, where high-speed flow channels produce higher plasma densities, not lower. The entering F region plasma there,

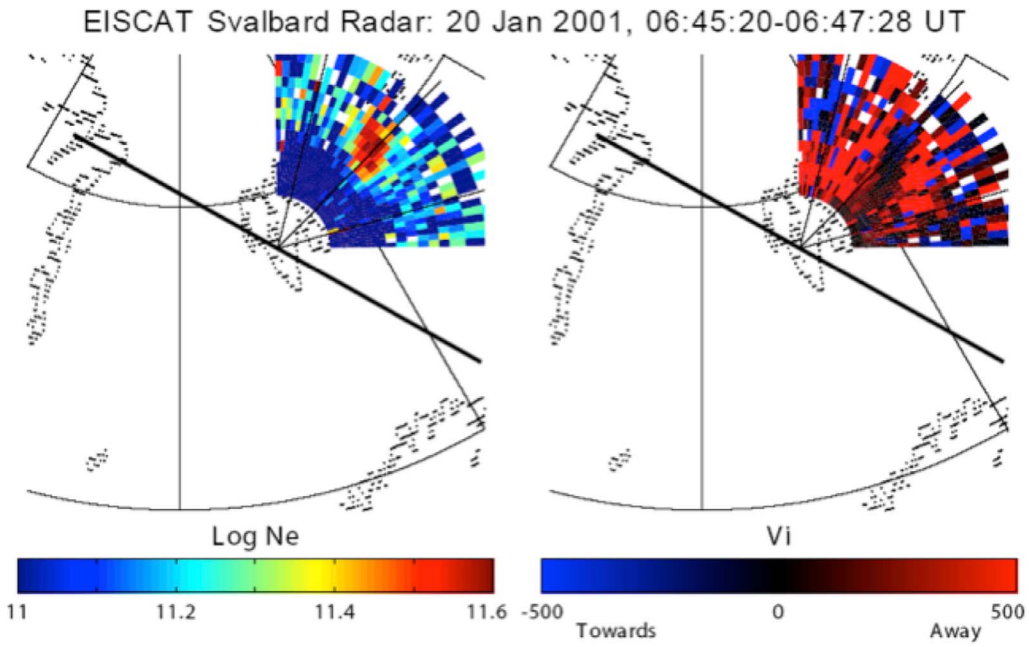

Figure 2. Creating an ISR capability to map areas ~600 km × ~1200 km in ~2 min [*Carlson et al.*, 2002] as shown here, enabled for the first time definitive testing of patch production mechanisms. (left) The log Ne plot shows a high-density patch (red central patch) immersed in low-density background plasma (blue). (right) The plasma velocity Vi shows a collocated strong plasma flow channel (blue-black) transporting plasma toward the ESR radar from a higher-density region, immersed in background opposite flow (red away from the radar) of lower polar cap plasma density (from *Carlson et al.* [2002]).

observed above 350 km, are above the reach of significant recombination by collisions of O+with neutral molecular nitrogen; this chemistry would apply to plasma near and below 250 km. The physics is correct, but at the altitudes at which the patches are observed. it is not relevant. Observations show this to be typical for at least the European sector.

[25] Next consider the magnetic reconnection mechanism for patch production proposed by *Lockwood and Carlson* [1992] involves reconnection at the magnetopause between the IMF and closed Earth magnetic field lines [*Cowley and Lockwood*, 1992] such that those closed field lines which would have been initially linked to corotating plasma in the ionosphere, subsequently are subject to transpolar flow within the polar cap boundary.

[26] This mechanism is subject to a severe logical test from ground based optics and ISRs, and was the driving force behind developing a high-speed wide area coverage ISR mode at the EISCAT Svalbard radar [*Carlson et al.*, 2002] as soon as its transmitter power became doubled. The physics of the reconnection event must lead to (1) initial dumping of trapped electrons (an almost immediate optical flash), then (2) within tens of seconds (electron gas heating time constant) the precipitating electrons must deposit heat into the electron gas to significantly raise its temperature absent significant other heat sources, then (3) within ~2 min (Alfven speed) the plasma will start to move in the IMF B_y magnetic tension direction, leading (4) the corotating plasma to instead move poleward (initially significant east/west component for appreciable B_y), and (5) within tens of seconds (ion thermal response time) frictional heating of Ti. These signatures must be present in this correct time sequence and relative spatial location to prove magnetic reconnection is at work [*Carlson et al.*, 2004]. If any of these signatures are absent or do not move/change in this relative temporal/spatial order, magnetic reconnection is shown not to be at play.

[27] Repeated observations such as illustrated in Figures 3 and 7 established this as the dominant mechanism [*Carlson et al.*, 2006] for at least in the European sector. No other mechanism leads to this distinctive set of signatures.

[28] Reconnection-driven patch generation injects corotating plasma into a trans–polar cap flow pattern, with the east-west component direction of the B_y magnetic curvature or "tension" force. Thus early patch injection follows the B_y magnetic curvature force direction, rapidly east or west (or directly poleward if $B_y \sim 0$), with B_y dependence as in Figure 4 (extrapolated from *Lockwood and Carlson* [1992]), and later as the magnetic tension relaxes the flow fades into the slower background antisunward flow.

3. Reversed Flow Events

[29] Plasma flow channels/jets, for B_z south conditions, always in the direction of the B_y tension force, have the signatures in ISR data as described just above. When seen in the dayside auroral region by other observing techniques they have been variously called: in meridian scanning photometers/imagers called PMFs or poleward moving auroral forms [see, e.g., *Sandholt et al.*, 2002]; in Super DARN poleward moving transients [*Milan et al.*, 2000]; in radar backscatter flow channel events (FCE) [*Pinnock et al.*, 1993]

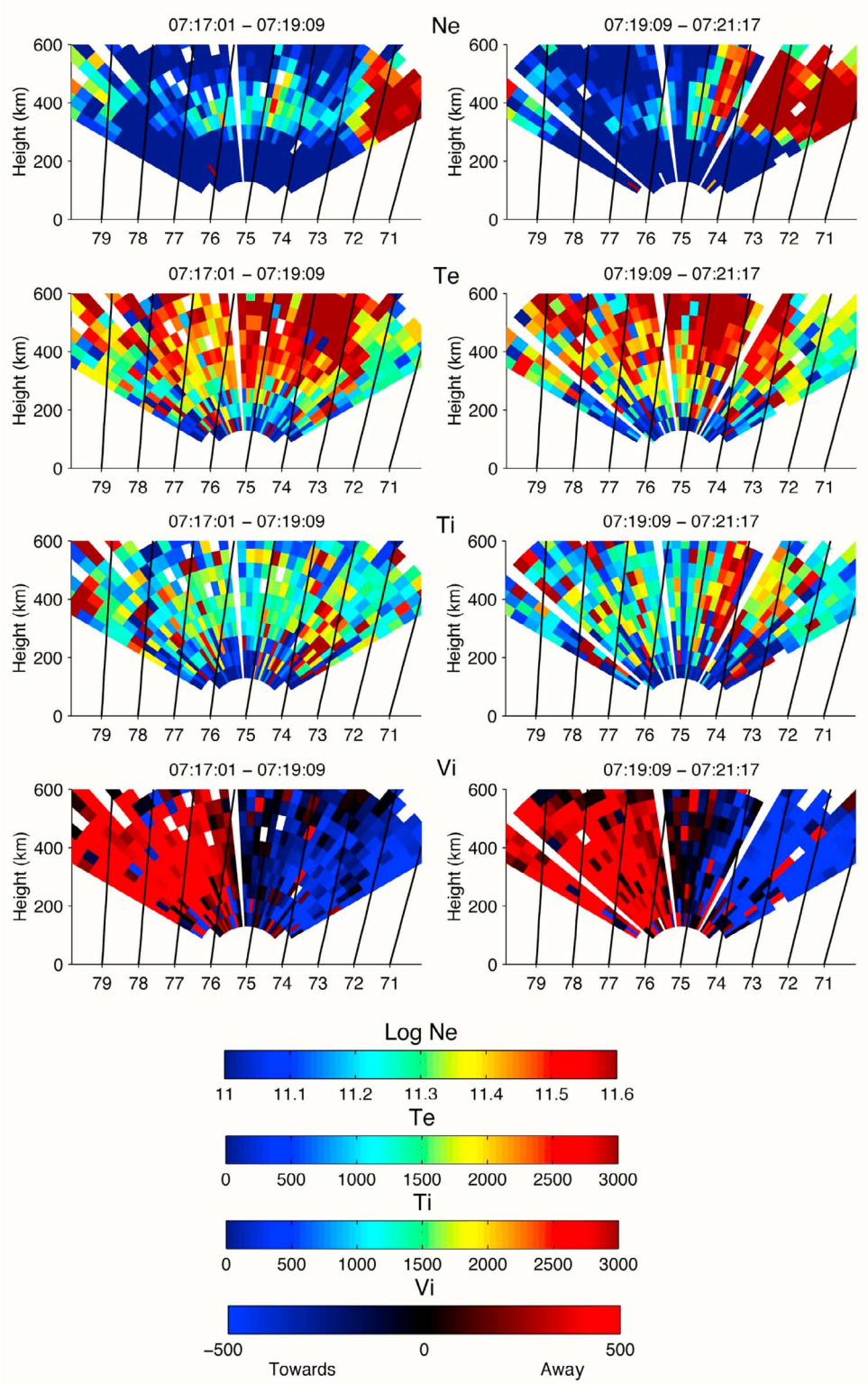

Figure 3. Detailed timing of optical flash followed by poleward leaps of Te, Vi, Ti, and Ne boundaries were able to prove magnetic reconnection to be the dominant strong-patch generation mechanism. Boundaries seen here in Ne, Te, Ti, and Vi jump poleward with the stringent time/space synchronism demanded by magnetic reconnection (from *Carlson et al.* [2006]).

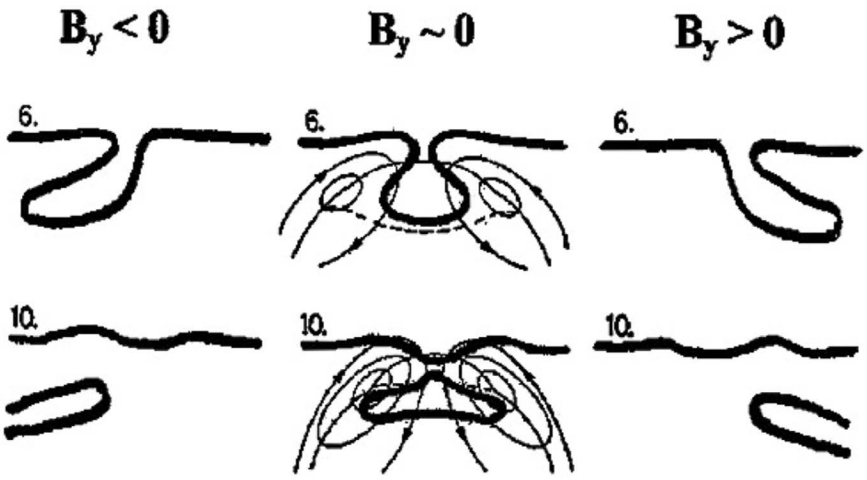

Figure 4. Patches born of magnetic reconnection follow a trajectory in time, in the *By*-dependent direction of the magnetic curvature/magnetic tension force as illustrated here (from *Carlson et al.* [2004] and extrapolated from *Lockwood and Carlson* [1992]). Here $Bz < 0$, the Sun is at the top, and the time progression designated by tx is for six and ten time steps after the instant of reconnection, where time of step 10 is greater than that of step 6. The thin lines under $By \sim 0$ are equipotential flow lines. By t 10 the first patch has separated into the polar cap, and the next reconnection event has initiated.

and poleward moving radar auroral forms (PMRAFs). These have been related in the satellite community to flux transfer events (FTEs). These features/signatures are often related to one another [e.g., *Moen et al.*, 2000].

[30] In sharp contrast to these, *Rinne et al.* [2007] discovered a new class of flow channels, which are characterized by flowing in the direction opposite the background flow, as illustrated in Figure 5. RFEs are ion flow channels

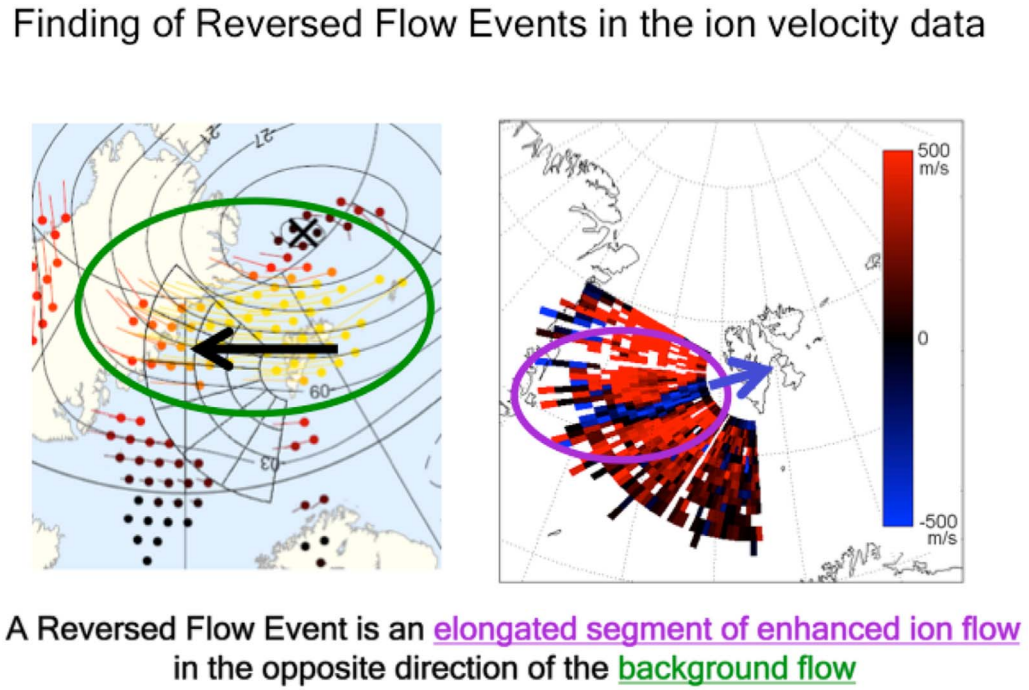

Figure 5. *Rinne et al.* [2007] discovered an entirely new class of cusp flow shears, where the transient flow is opposite that of magnetic tension, called reversed flow events (RFEs). (left) Plasma flow measured by SuperDARN showing general westward flow (black arrow) and (right) ESR plasma flow measurements of a narrow channel of eastward (reversed) flow (blue channel and blue arrow) in the center of the general westward flow (red). The black lines in Figure 5 (left) outline the ESR field of view. Study of ISR mapping scans showed RFEs occur half the time within 1 h about 12:30 MLT, very rarely outside this time, and independent of *Bz* and *By*. (Based on figure from *Rinne et al.* [2007].)

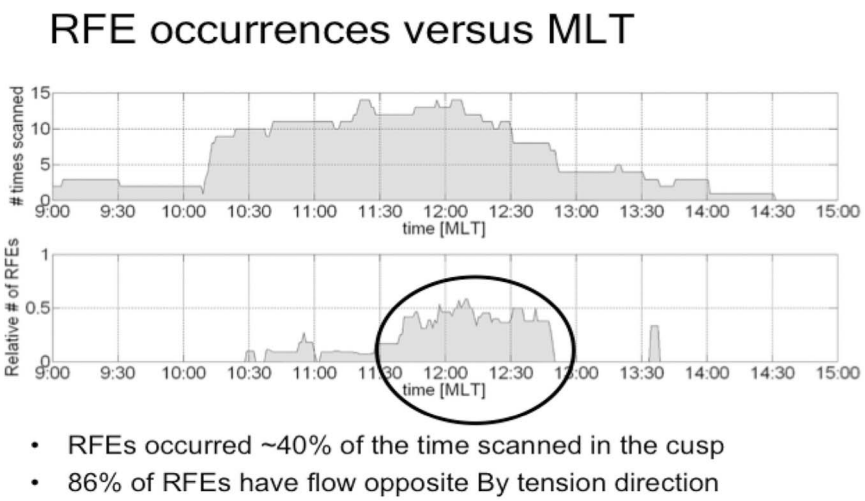

Figure 6. Occurrence rate versus MLT (magnetic local time) of RFEs discussed in text and Figure 5. (Based on figure from *Rinne et al.* [2007].)

generally opposite to the IMF *By* controlled magnetic tension pull on newly opened field lines, and opposite the larger-scale background hence the name Reversed Flow Events. They are longitudinally elongated flow channels (>400–600 km) that oppose the large-scale background flow in the cusp region, typically ∼50–250 km wide, within which the flow speed is >250 m/s (often much larger). Their lifetime averaged ∼19 min.

[31] Figure 6 summarizes the results of analysis of 767 ISR mapping scans from 11 winter days within 09:00–14:30 UT. RFEs ion flow was in 95% of the cases documented to oppose the magnetic tension force, and cannot be interpreted in terms of newly opened flux. The occurrence rate was independent of B_z and B_y, occurred for clock angles of 40–240°, and were seen half the time during 1 h centered on 12:30 MLT but <10% to 0% outside this time. *Moen et al.* [2008] have related these to narrow Birkeland current sheets, but their physics is not fully understood. Aside from channel width, length, and lifetime similar to reconnection events, RFEs are distinctly different. However, consequences of the flow shears they drive can lead to very similar physical consequences. *Oksavik et al.* [2011] have now detected signatures of this phenomenon with SuperDARN techniques.

4. Patch Structuring

[32] We have found that the dominant mechanism for producing patches is magnetic reconnection, as supported by the five points in the section above on Patch Formation Injection. Departure from the presence of all five criteria noted, all in the relative temporal and spatial order specified, would rule out this mechanism. Events observed with adequate time resolution (about 2 min), spatial coverage (∼600 × 1000 km), and needed coincident parameter (Te, Ti, Ne, Vi, and ideally photometric optical data), repeatedly meet all these very stringent requirements [e.g., *Carlson et al.*, 2002, 2004, 2006, 2007, 2008; *Oksavik et al.*, 2005; *Moen et al.*, 2004]. We thus are led to view strong plasma sheers as inherent in patch creation, at least in the European sector.

[33] If in other longitude sectors velocity dependent recombination should be found to be important to segmenting tongues of ionization entering the polar cap into patches, these likewise have strong plasma flow sheers inherent in that patch production mechanism. Likewise even if reverse flow events should be found to yield a patch.

[34] With strong plasma sheers inherent in patch production, why then is patch structuring believed to be dominated by the gradient drift (GD) instability, not the shear driven instability? The later has a much faster onset time. To pursue this question, obvious once one realizes shears are intrinsic to patch creation, an experiment was done [*Carlson et al.*, 2007] to directly resolve the question. A series of successive patches were traced from eruption out of corotation, to poleward motion overhead two downstream locations spaced such as to define instability risetimes.

[35] With the EISCAT Svalbard Radar (ESR) scanning magnetic north-south from near the north coast of Norway to near the northwest coast of Greenland with two minute resolution; the mainland UHF Tromso radar pointed in a fixed poleward direction with one minute resolution. Figures 7a–7d show the ESR north-south Ne cross sections of high-density (red) corotating sunlit plasma south of 72.5° latitude and low-density (blue) polar Ne poleward of that, at 07:18 UT. By 07:20 UT the high-density Ne boundary has leaped over 200 km poleward. This coincides with a coincident optical poleward moving auroral form (PMAF) flash, seen in Figures 7e–7l showing ASIP (all sky imaging photometers) 777.4 nm emission overhead images. At 07:16 UT in Figure 7a, the high-density Ne just south of overhead is the remains of the prior patch about to move out of the plane of the ESR scan. Tromso data along the low-elevation line of sight from Tromso in Figure 8 show a like coincident poleward leap of Vi, Te, and Ti and boundaries for a train of five clear such events 07:00–07:40 UT. PMAFs in 630.0 nm are seen in the fifth panel, and Ne in the second panel. The sixth panel in Figure 8 shows 5 patches of Ne breaking poleward from corotation near 72.5° latitude and passing over Lonyearbyen (LYR), then NyAlesund (NYA), at time delays matching Vi measured from Tromso. Scintillation

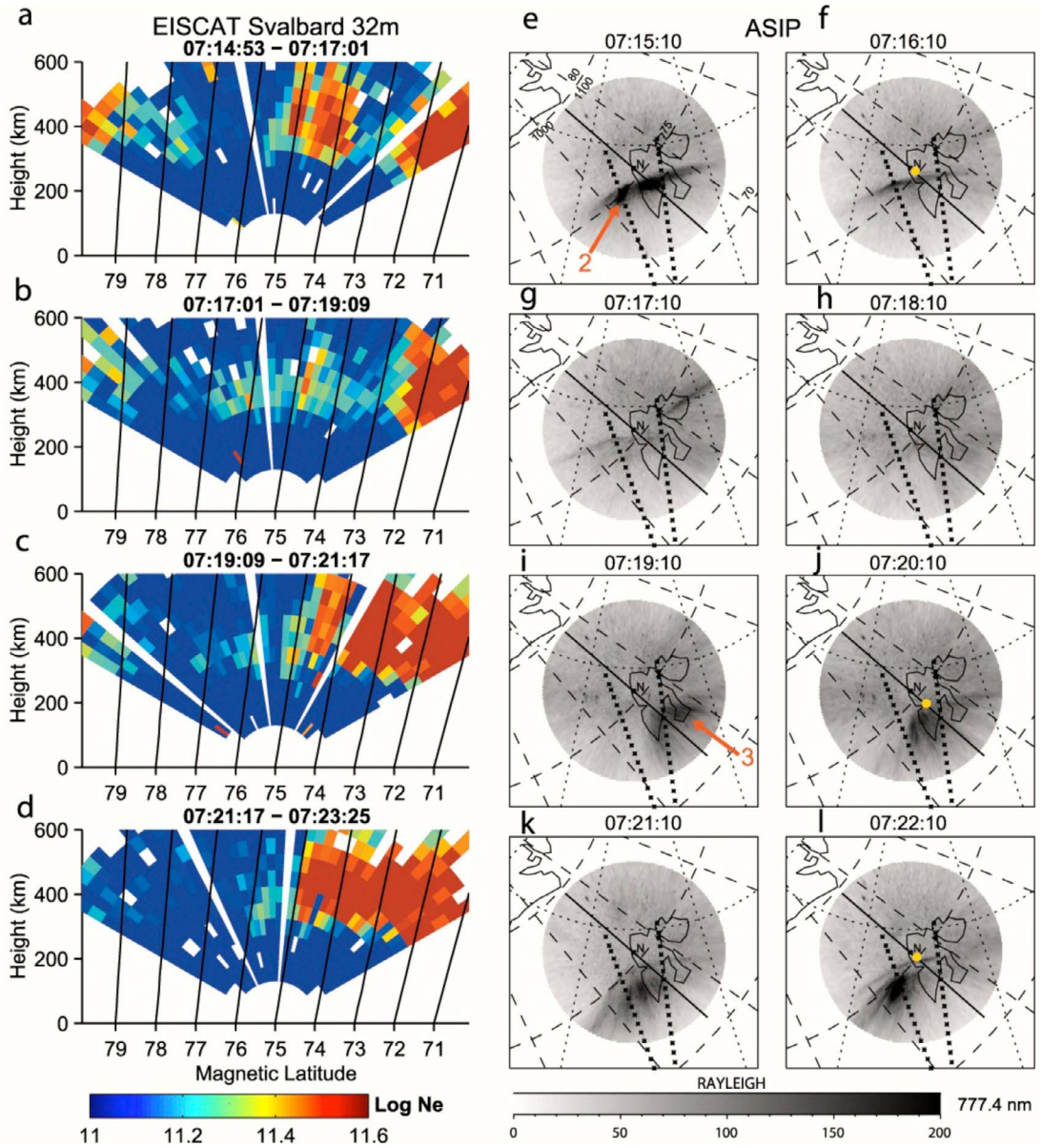

Figure 7. Time progression of patch injection seen in a north–south plane: (a) an Ne patch ~74°–75° MLat (red) already in the background low Ne density (blue) polar cap, which erupted from corotating solar produced plasma near the edge of the cusp ~72° MLat; (b) the instant before the next patch is created; and (c and d) tracking of poleward injection of the next high-density Ne (red) patch with poleward boundary seen near 75° MLat. (e–h) Coincident 777.7 nm 1 min resolution optical images track "PMF" signatures of poleward/westward motion of associated optical signatures of the Ne patch in Figure 7a, and (i–l) the next Ne patch (Figures 7c and 7d) erupting from the corotating plasma near and below 72° MLat (Figure 7b) is tracked. Red arrows refer to second and third patch in a series of 5 seen in Figure 8 [after *Carlson et al.*, 2006].

receivers at each of these two sites measure five bursts of scintillation, one burst each time one of the patches passes overhead. The patches yield strong scintillation (S4 ~ 0.8) over LYR and saturated S4 over NYA two minutes downstream from LYR. *Carlson et al.* [2007] calculated the expected instability rise and onset times for the shear driven instability, matching those observed at both stations. The time calculated for the GD instability was far longer than observed. Patches are in truth structured on creation by shears, not the DG instability!

[36] First, upon injection of corotating plasma into transpolar flow, the plasma is in a rapid flow channel, and the shear driven instability sets in within a few minutes, not the previously believed 10–15 min. At this time the flow is typically ~2 km/s, and the patch rapidly structures throughout. After ~15 min, the magnetic tension force relaxes, and the patch flow relaxes into the general background transpolar flow of ~0.5–1 km/s. At this time downstream in the polar cap, shear no longer applies, and GD [*Keskinen and Ossakow*, 1983] is

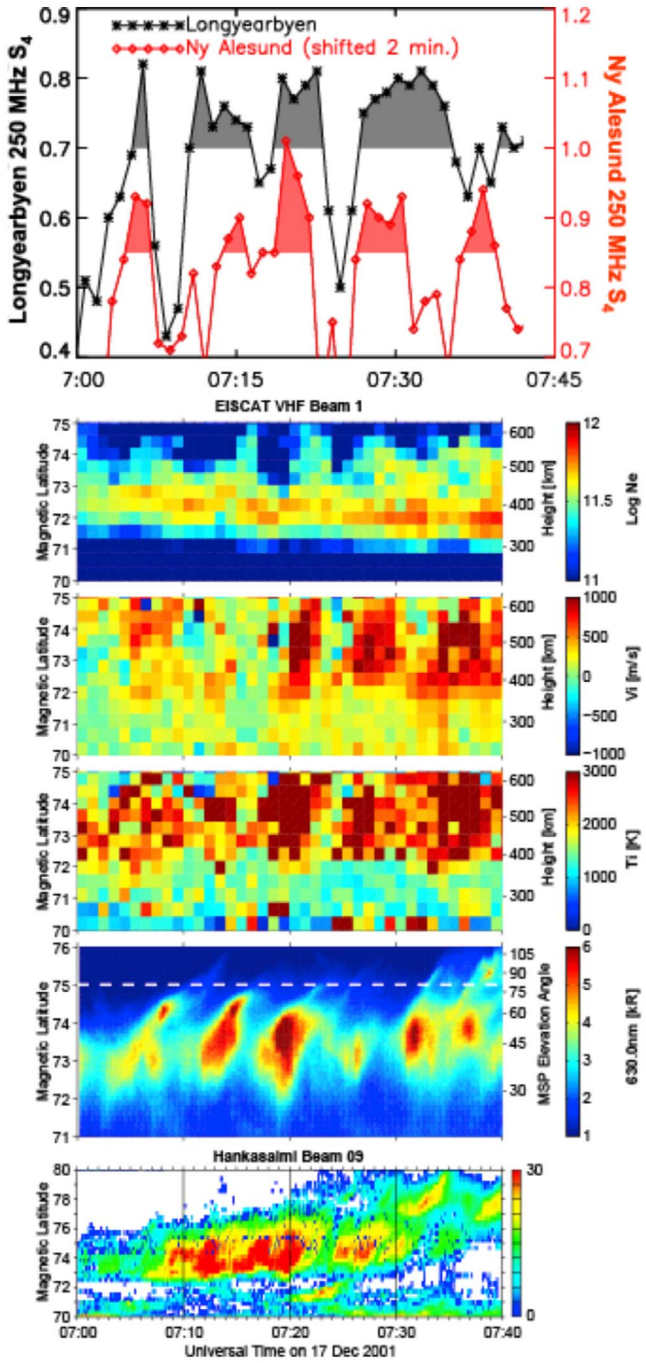

Figure 8. Detailed tracking of five successive patches from corotation through injection into the polar cap, seen in Ne, Ti, and Vi, and 630.0 nm "PMFs" in the second, third, fourth, and fifth panels [*Carlson et al.*, 2006, 2007]. The first panel shows scintillation S4 measured at LYR and NYA 200 km farther downstream from the cusp. The instability risetime, minutes for five successive patches, proves the shear driven instability, not the much slower gradient drift instability believed for 20 years to dominate [*Carlson et al.*, 2007]. The sixth panel illustrates that 6 m scale irregularities also cascade from the larger-scale irregularities [*Carlson et al.*, 2008]. (Composite from *Carlson et al.* [2006, 2007, 2008].)

left to dominate maintenance of structuring the plasma as it moves toward the nightside auroral oval. This has been verified in the central polar cap [*Basu et al.*, 1990]. Upon exiting, if by magnetic reconnection, shear driven structuring may again apply. This explains many previously unexplained observed properties of cusp and polar cap patches.

[37] For two decades it had been believed that, while the shear driven instability dominated plasma structuring for northward IMF conditions, the gradient drift instability dominated all plasma structuring for southward IMF conditions. Now we have learned that while the latter dominates in the central polar cap, future theory and modeling must adopt the new framework or two-step process described here, to correctly represent patch structuring entering and transiting the polar cap. Otherwise we can be 5–10° of latitude in error as to where comm./GPS are at risk. The onset of strong-to-saturated scintillation within minutes and a few hundred km of the cusp, versus 10–20 min and 600–1000 km of the cusp, is one dramatic recent finding.

[38] The next question this now raises is, down to what scale size does the plasma structure? Is there cascading of even smaller scale structures off larger scales? Scintillation observations measures from ~100 km down to ~100 m scale irregularities. Do irregularities extend farther down by another order of magnitude to ~10 m scale. *Carlson et al.* [2008], by adding SuperDARN data to that from the ESR, as shown here in the sixth panel of Figure 8, indicated yes. The data in Figure 9 [*Moen et al.*, 2000] shows the consistency of their initial findings. *Oksavik et al.* [2011] published firm confirmation. For a shear driven phenomenon as we have found, one would expect with some growth rate (whose theory is yet to be developed down to these scales), structure and echoes would develop along the shear lines. Consequently echoes should be Doppler broadened by the "turbulent mixing" over scales larger than 10 m, and thus one should consequently expect to detect the often seen Doppler PMF broadening shift. More focused work needs to be done, with care for spatial/temporal resolution/coincidence before observations can give meaningful guidance to further theoretical development.

[39] What can be confidently said now however is illustrated here in Figure 9. *Moen et al.* [2000] pointed out that Superdarn echoes have a faster onset than expected from GD. The findings here about the shear driven instability can explain this rapid echo onset time in Figure 9 if the cascade process down to ~10 m has similarly rapid growth. Figure 9 thus dramatically illustrates how rapidly the cusp can fill with widespread irregularities, scintillation, and a comm./nav. outage region (successive frames are minutes apart over an area order 500 × 1000 km).

[40] The new framework for polar cap plasma structuring, scintillation, and satellite outages [*Carlson et al.*, 2007] must recognize that the shear driven instability drives plasma structuring in not only polar cap arcs, but dominates rapid structuring of newly created patches; while the gradient drift (GD) instability becomes dominant ~15 min downstream to maintain patch structuring deeper in the polar cap. Outage onset is faster/closer than previously recognized.

5. Patch Trajectory

[41] Our understanding of the transit of patches across the polar cap to exit on its nightside, has also been significantly

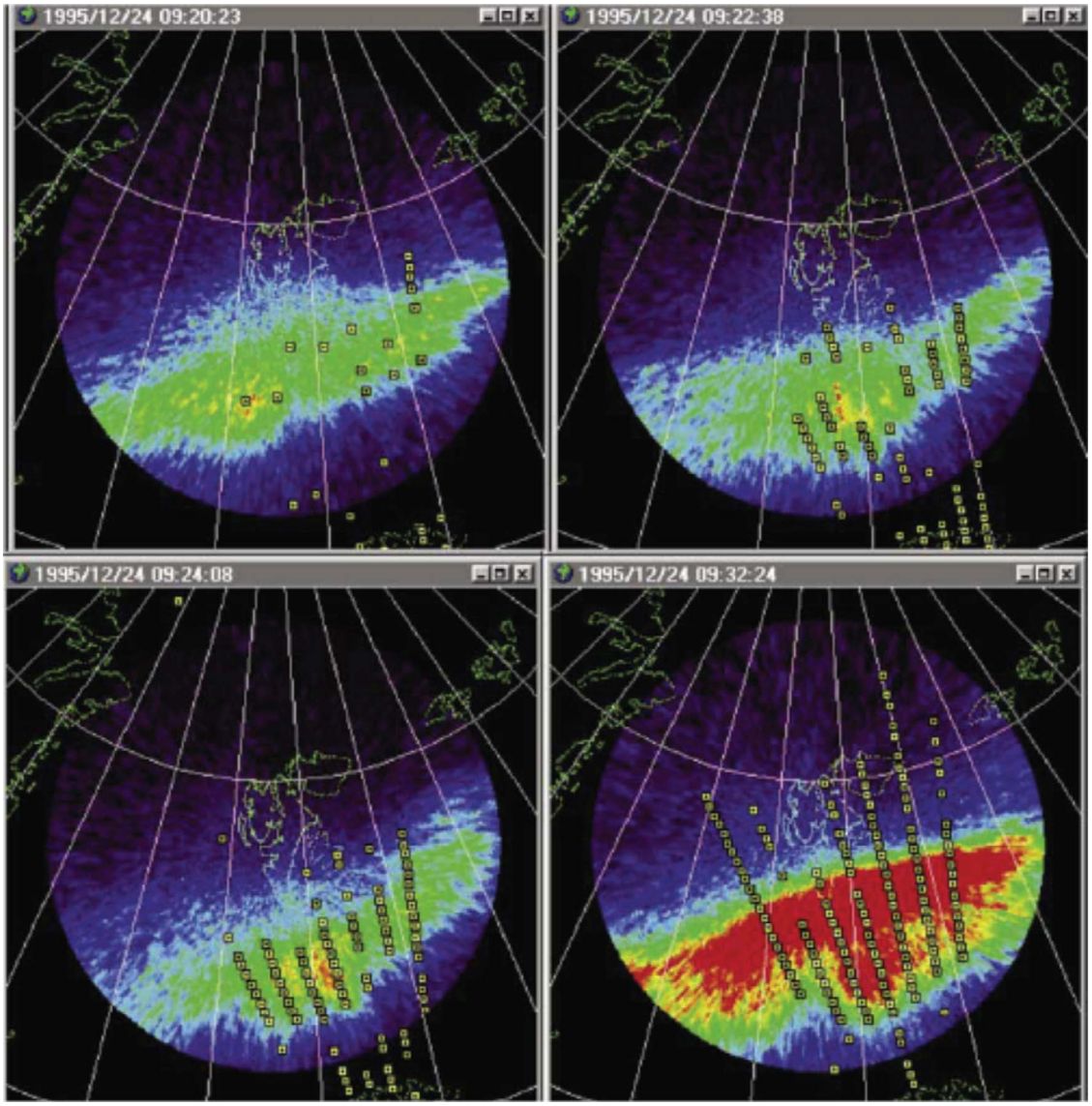

Figure 9. Because shear driven instabilities, not GD, cause initial patch structuring within minutes of patch creation, *Carlson et al.* [2008] further hypothesized and gave evidence confirmed by *Oksavik et al.* [2011] that that rapid cascading of scintillation-producing irregularities down to ~10 m scale structure can explain the explosive (minutes) onset of SuperDARN scale structuring, to which *Moen et al.* [2000] first called compelling attention, as dramatically illustrated here. Such techniques thus can quickly map the onset of large areas at risk of disruption of RF services (scintillation, HF, GPS, etc.) (from *Moen et al.* [2000]).

extended by *Moen et al.* [2007], who analyzed eight Northern Hemisphere winter season's data have tracked patch trajectories toward their nightside exit from the polar cap, as seen here in Figure 10. They have not only demonstrated proof of concept for detecting and tracking patches exiting the polar cap, but documented enough cases to give clear experimental guidance for better morphological representation of actual paths of patches across the nightside polar cap. Exit is found to be over a wider range of local times than many had previously thought. Further, an apparent poleward leap of the auroral poleward boundary to "meet" the exiting patch optical signature, supports the idea that patch exit also involves magnetic reconnection.

[42] *Oksavik et al.* [2010] show how patches of high electron density measured by ESR and associated with patches of SuperDARN radar backscatter can track across the polar cap and then reappear in a radar on the nightside.

6. Thermospheric Consequences

[43] Viewing magnetic reconnection as the dominant mechanism producing patches, for reasons noted above in Patch Formation/Injection and Patch Structuring, not only logically leads as discussed in Patch Structuring to closer examination of the dominant driver of plasma structuring during the high-velocity phase of patch insertion into the

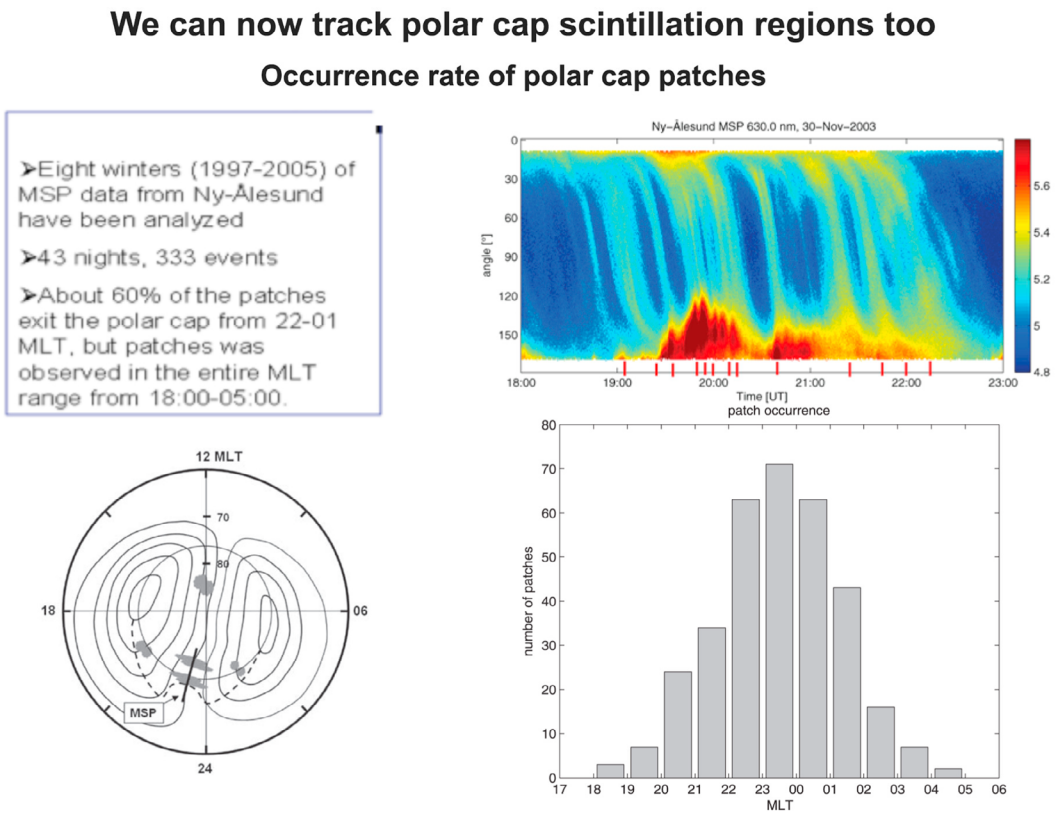

Figure 10. Trajectories of patches as they approach exiting the nightside polar cap as seen here give new insight to trajectory, exit morphology, and physics of patch exit. (Based on figures from *Moen et al.* [2007]).

polar cap, and consequent revision of our framework for understanding of polar patch structuring. It equally logically calls for examination of the thermospheric response to such transient plasma flow jets, and thus to be expected frictional drag heating events.

[44] *Lühr et al.* [2004] called the attention of the community to significant thermospheric density and temperature perturbation over the cusp by publishing neutral drag/density enhancements up to a doubling, over the cusp. They correctly suggested upwelling from joule heating as an explanation. Prior to that time the only other paper in the literature addressing thermospheric heating response in the cusp was by *Carlson* [1998]. It pointing out that the thermospheric response to joule/frictional heating in the cusp was fundamentally dramatically greater than over the midnight aurora, for four specific physics reasons which all conspired to reinforce each other. After the dramatic observations by *Lühr et al.* [2004], *Carlson* [2007] applied these four compounding principles to quantitatively reproduce, for an overhead cusp, an up to doubling or cusp thermospheric densities with joule heating. The connection to joule heating, as suggested by *Lühr et al.* [2004], and that this heating is triggered by magnetic reconnection events as suggested by *Carlson* [2007], is supported by two further findings in the literature. First is the fact that flow shears are ubiquitous near the cusp [e.g., *Neudegg et al.*, 2000; *McWilliams et al.*, 2000]. Also, fine structure currents are so typical of these shears, associated with magnetic reconnection, that it has been suggested to call them a new current system associated with the cusp [*Oksavik et al.*, 2005].

[45] The four essential elements of physics distinguishing heating of the cusp thermosphere [*Carlson*, 1998, 2007] are (1) where the flow channel is several neutral scale heights wide, the primary thermospheric expansion is upward; (2) low-energy cusp particles lead the joule heating to be deposited at higher altitudes (than night side auroral particles) where energy dissipation of currents is dissipative versus nondissipative; (3) the thermospheric response to energy deposition increase rapidly with altitude (the thermosphere is ~100 more tenuous near 200 km than near 110 km); and (4) joule heating is proportional to the square of the electric field E or ion velocity relative to neutrals. Scaling from *Valladares and Carlson* [1991] and *Ma and Schunk* [1997], *Carlson* [2007] calculated up to ~80% density enhancements at the 400 km altitude, as observed by *Lühr et al.* [2004].

[46] *Thayer and Semeter* [2004] help put this in perspective. Among others they illustrate that Joule heating at high latitudes often exceeds particle heating. Significantly, *Thayer and Semeter* [2004, appendix] furthermore present a clear explanation of why Joule heating in the altitude range ~140 through hundreds of km, can be equivalently expressed in term of frictional ion heating. This in turn depends on the square of the ion velocity in the neutral rest frame, $(Vi–Vn)^2$. Critical is that calculations be based on height

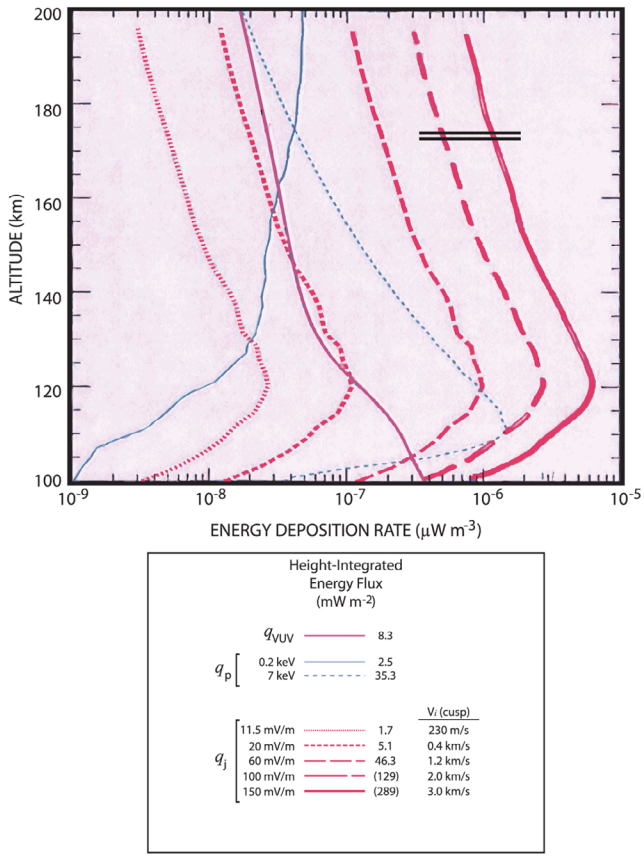

Figure 11. Profile of energy deposition rate, after *Thayer and Semeter* [2004], but adding higher energy deposition rates for 2 km/s and 3 km/s, conditions more representative of transient flow shears in magnetic reconnection regions, as well as other observed polar flow transients. These lead to significantly greater cusp heating than currently generally recognized. (Modified after *Thayer and Semeter* [2004], copyright 2004, with permission from Elsevier).

integrated profiles, accurately tied to Ne(h) input. We reproduce the altitude resolved energy deposition rate from *Thayer and Semeter* [2004, Figure 2], and will add a few further profiles to it here augmented to be our Figure 11. In this figure q_{VUV} is solar VUV energy deposition rate for the conditions they describe at Sondre Stromfjord Greenland, q_p is the particle energy deposition rate for their representative hard and soft auroral particle precipitation as labeled in the figure, and their remaining curves present ion frictional heating for three representative high-latitude electric fields. They also list height integrated energy flux for each case. We have added labels of the equivalent Vi–Vn, namely 230 m/s, 0.4 km/s, and 1.2 km/s. The later two are representative of average transpolar flow in the central polar cap [e.g., *Heelis*, 1984].

[47] It is only during the initial phase (~15 min) of reconnection the flow channel is of unusually high speed (~2–3 km/s), then flow relaxes downstream into the background transpolar flow pattern (~0.5–1 km/s). The initial high-speed flow channel should be expected to significantly heat the overhead thermosphere, and this has been quantified with overhead calculations showing that it does [*Carlson*, 2007]. Surprising has been the subtlety/difficulty of achieving a good quantitative global-scale modeling calculation of the thermospheric heating and response. *Demars and Schunk* [2007], in their model calculations to match the observed *Lühr et al.* [2004] thermospheric response at 400 km, had to increase their energy deposition rate by a factor of about two orders of magnitude, an amount leading the community to discount this modeling which exposed several other pieces of valuable circulation cell physics. Other global modeling efforts have likewise continued to not be accepted. Elements of our improved understanding of the cusp have contributions to make here too.

[48] It is not uncommon to observe transient 2–3 km/s flow shears near the cusp at patch initiation; such velocities are also seen by DMSP [*Carlson et al.*, 2007; *Valladares et al.*, 2002]. We thus add to Figure 11, two additional frictional heating profiles of energy deposition rate calculated (scaled up) for ion plasma velocities of 2 km/s and 3 km/s. Applicable data for testing consequences are from winter near Svalbard. There typical altitude profiles Ne(h) show a plasma density ledge with Ne falling sharply below ~180 km. Thus we draw a line at this height in Figure 11, below which the energy deposition rate would significantly drop for these conditions. We accordingly put parentheses around the height integrated energy flux, which would be correspondingly reduced an order of magnitude for the linear dependence on Ne (as per equations in *Thayer and Semeter* [2004, appendix]).

[49] The thermospheric response would not change significantly for heating only above ~180 km, to first order the isopicnic point would move up from 120 km to 180 km, and the enhanced neutral temperature and scale height would then apply for the remaining many scale heights integrated up to 400 km, essentially as scaled/calculated from *Valladares and Carlson* [1991] and *Ma and Schunk* [1997] and by *Carlson* [2007]. However, removal of the integrated energy deposition below 180 km would then be very significantly reduced, as evident from the energy deposition rate profiles below 180 km in Figure 11. This then would significantly reduce objections raised to an excessive height integrated energy flux used by [*Demars and Schunk*, 2007] in their model calculations, to match the observed *Lühr et al.* [2004] thermospheric response at 400 km. Reduction of energy deposition by an order of magnitude (energy above 180 vs 120 km), and transiently increasing energy deposition rates an order of magnitude (3 vs 1 km/s), is two orders of magnitude.

[50] Because the ion velocity shear is transient and narrow, the thermospheric wind does not have time to come up to speed in a given event, so Vi shear is the key measurement. The range of velocity shears observed, and typical Ne(h) observed, "predicts" the range of cusp density enhancements well matched to those observed [*Lühr et al.*, 2004]. Such enhancements should not be limited to the cusp, strong shears are seen elsewhere. The net consequences for the cusp and polar cap thermosphere, depends on altitude profiles, spatial/temporal extent, and event frequency. Analysis now in progress indicates that beyond individual local thermpospheric temperature and density enhancements, the sum of such events is enough net energy to need consideration in the overall thermal balance of the polar thermosphere.

[51] Shears near the cusp are ubiquitous, frequent, extensive, and persist long enough call for study as a heat source to the polar thermosphere. Typical magnitudes (2–3 km/s), horizontal extent (~1000 km), and persistence (>10 min) are documented in *Oksavik et al.* [2005] and *Carlson et al.* [2007]. The database on which IRI Ne(h) is based in the dark cusp is sparse.

[52] In a nutshell, Poynting Flux is the incoming EM energy available for conversion into thermospheric heating, plasma densities below 200 km (where particle production is key in the dark cusp region) is key to the altitude at which this energy is deposited, and the thermospheric response is critically dependent on how high this altitude is. Going fro hard to soft particle flux, or from 120 km to 180 km, has order of magnitude consequences. Beyond individual events, the cumulative affect on the polar thermosphere should not be neglected.

7. System Implications

[53] Many by now have come to consider the space environment as inherently a part of any satellite system. Operations would be aided by more exposure to this understanding. From any perspective, several of the new discoveries reviewed here have clear impact on space communications, navigation, data links, and space situational awareness in terms of upper atmospheric densities and perturbations of satellite drag.

[54] Plasma irregularities/instabilities that can lead to disruptive scintillation occur near the dayside auroral region, and occur with much smaller lead time and at lower latitudes than previously thought. New knowledge of their signatures can help better mitigation techniques. Downstream potential outage regions move over a wider range of paths than thought, but tracking techniques can be devised. Satellite drag models need to add a new heating process for improved now-forecast. HF communications and radar clutter are also impacted by these new findings and can benefit from incorporation of them into future thinking.

8. Conclusions

[55] We have endeavored here to follow a line of logical linkage from one finding to the next, to make many of the more recent discoveries unfold as virtually inevitable consequences of earlier steps. For example flow shears of any origin can lead to several linked consequences including: enhanced plasma structuring driven by the shear-driven instability; faster scintillation onset; previously unexpected HF scatter from secondary irregularities feeding off primary structure born of the shear driven instability; frictional drag heating of the lower thermosphere; enhanced satellite drag perturbations in the upper thermosphere.

[56] Our key conclusions are:

[57] 1. Magnetic reconnection dominates strong patch production [*Carlson et al.*, 2004, 2006], while weak patches are additionally produced by particles in the cusp [*Pinnock et al.*, 1995; *Rodger et al.*, 1995] and polar cap [*Oksavik et al.*, 2006].

[58] 2. This dominant source inserts high-density plasma into polar cap by injecting flow in the magnetic tension direction with initial flow ~2 km/s.

[59] 3. Strong plasma flow shears are inherent in this mechanism creating most patches; incorporating this into a new framework is required if we are to adequately model/predict several aspects of the satellite environment.

[60] 4. Another class of shears has been discovered in the cusp, confined to ~ an hour near noon MLT, called reverse flow events (RFEs), usually flowing opposite the magnetic tension direction.

[61] 5. Structuring of patches on first entering the polar cap is not by the gradient drift instability as believed for decades. The shear driven instability first fully structures the patch during its first 15 min upon entering the polar cap, the gradient drift instability dominates later when the patch is downstream deeper in the polar cap. This underlying physics applies not only to magnetic reconnection driven flow shears, but flow shears more generally (e.g., RFEs and other flow shears).

[62] 6. This in turn means scintillation onset is much more rapid and closer to the cusp than previously known.

[63] 7. Shear driven irregularities at scales producing scintillation, are observed to further lead to smaller-scale ~10 m scale structure and radar scatter over similar scales, through plasma processes in need of further theoretical refinement.

[64] 8. The downstream patch (outage region) trajectory traverses and exits the polar cap over a much wider range of MLTs than previously known.

[65] 9. Plasma shears inherent in patch production can have significant effects on thermospheric densities, creating long ridges of neutral density enhanced by ~10s–100% near 400 km (satellite speed bumps in the sky),

[66] 10. Cumulatively over the polar cap this transient heating, stemming from plasma flow shears, adds up to a new polar thermospheric heat source that cannot be ignored.

[67] **Acknowledgments.** The author gratefully acknowledges a long-standing close working relationship with colleagues at AFRL and with J. I. Moen, K. Oksavik, and Y. Rinne for a rich decade of shared exciting joint discovery. This review of work, in large part born of that rich collaboration, has been sponsored by the Utah State USTAR innovative initiative program at SWC, USU. EISCAT is an international association supported by Finland (SA), France (CNRS), the Federal Republic of Germany (MPG), Japan (NIPR), Norway (NFR), Sweden (NFR), and the United Kingdom (PPARC).

References

Anderson, D. N., J. Buchau, and R. A. Heelis (1988), Origin of density enhancements in the winter polar cap, *Radio Sci.*, *23*, 513–519, doi:10.1029/RS023i004p00513.

Anderson, D. N., D. T. Decker, and C. E. Valladares (1996), Modeling boundary blobs using time varying convection, *Geophys. Res. Lett.*, *23*, 579–582, doi:10.1029/96GL00371.

Basu, S., and C. E. Valladares (1999), Global aspects of plasma structures, *J. Atmos. Sol. Terr. Phys.*, *61*, 127–139, doi:10.1016/S1364-6826(98)00122-9.

Basu, S., E. MacKenzie, S. Basu, E. Costa, P. F. Fougere, H. C. Carlson, and H. E. Whitney (1987), 250 MHz/CHz scintillation parameters in the equatorial, polar and auroral environments, *IEEE Trans. Commun.*, *5*, 102–115.

Basu, S., E. MacKenzie, and S. Basu (1988a), Ionospheric constraints on VHF/UHF communications links during solar maximum and minimum periods, *Radio Sci.*, *23*, 363–378, doi:10.1029/RS023i003p00363.

Basu, S., S. Basu, E. MacKenzie, P. F. Fougere, W. R. Coley, N. C. Maynard, J. D. Winningham, M. Sugiura, W. B. Hanson, and W. R. Hoegy (1988b), Simultaneous density and electric field fluctuation spectra associated with velocity shears in the auroral oval, *J. Geophys. Res.*, *93*, 115–136, doi:10.1029/JA093iA01p00115.

Basu, S., S. Basu, E. MacKenzie, W. R. Coley, J. R. Sharber, and W. R. Hoegy (1990), Plasma structuring by the gradient drift instability at

high latitudes and comparison with velocity shear driven processes, *J. Geophys. Res.*, *95*(A6), 7799–7818, doi:10.1029/JA095iA06p07799.
Carlson, H. C. (1994), The dark polar ionosphere: Progress and future challenges, *Radio Sci.*, *29*, 157–165, doi:10.1029/93RS02125.
Carlson, H. C. (1998), Response of the polar cap ionosphere to changes (solar wind) IMF, in *Polar Cap Boundary Phenomena*, edited by J. Moen, A. Egeland, and M. Lockwood, pp. 255–270, Kluwer Acad., Dordrecht, Netherlands.
Carlson, H. C. (2007), Role of neutral atmospheric dynamics in cusp density and ionospheric patch formation, *Geophys. Res. Lett.*, *34*, L13101, doi:10.1029/2007GL029316.
Carlson, H. C., K. Oksavik, J. Moen, A. P. van Eyken, and P. Guio (2002), ESR mapping of polar-cap patches in the dark cusp, *Geophys. Res. Lett.*, *29*(10), 1386, doi:10.1029/2001GL014087.
Carlson, H. C., K. Oksavik, J. Moen, and T. Pedersen (2004), Ionospheric patch formation: Direct measurements of the origin of a polar cap patch, *Geophys. Res. Lett.*, *31*, L08806, doi:10.1029/2003GL018166.
Carlson, H. C., J. Moen, K. Oksavik, C. Nielsen, I. W. McCrea, T. Pedersen and P. Gallop (2006), Direct observations of injection events of subauroral plasma into the polar cap, *Geophys. Res. Lett.*, *33*, L05103, doi:10.1029/2005GL025230.
Carlson, H. C., T. Pedersen, S. Basu, M. Keskinen, and J. Moen (2007), Case for a new process, not mechanism, for cusp irregularity production, *J. Geophys. Res.*, *112*, A11304, doi:10.1029/2007JA012384.
Carlson, H. C., K. Oksavik, and J. Moen (2008), On a new process for cusp irregularity production, *Ann. Geophys.*, *26*, 2871–2885, doi:10.5194/angeo-26-2871-2008.
Coley, W. R., and R. A. Heelis (1998), Structure and occurrence of polar ionization patches, *J. Geophys. Res.*, *103*, 2201–2208, doi:10.1029/97JA03345.
Cowley, S. W. H., and M. Lockwood (1992), Excitation and decay of solar wind-driven flows in the magnetosphere-ionosphere system, *Ann. Geophys.*, *10*, 103–115.
Crowley, G. (1996), A critical review of ionospheric patches and blobs, in *Review of Radio Science 1993–1996*, pp. 619–648, Oxford Univ. Press, New York.
Dandekar, B. S., and T. W. Bullett (1999), Morphology of polar-cap patch activity, *Radio Sci.*, *34*, 1187–1205, doi:10.1029/1999RS900056.
Demars, H. G., and R. W. Schunk (2007), Thermospheric response to ion heating in the dayside 398 cusp, *J. Atmos. Sol. Terr. Phys.*, *69*, 649–660, doi:10.1016/j.jastp.2006.11.002.
Foster, J. C. (1993), Storm time plasma transport at middle and high latitudes, *J. Geophys. Res.*, *98*, 1675–1689, doi:10.1029/92JA02032.
Foster, J. C., et al. (2005), Multiradar observations of the polar tongue of ionization, *J. Geophys. Res.*, *110*, A09S31, doi:10.1029/2004JA010928.
Heelis, R. (1984), The effects of interplanetary magnetic field orientation on dayside high-latitude convection, *J. Geophys. Res.*, *89*, 2873–2880, doi:10.1029/JA089iA05p02873.
Keskinen, M. J., and S. L. Ossakow (1983), Theories of high-latitude ionospheric irregularities: A review, *Radio Sci.*, *18*(6), 1077–1091, doi:10.1029/RS018i006p01077.
Lockwood, M., and H. C. Carlson (1992), Production of polar cap electron density patches by transient magnetopause reconnection, *Geophys. Res. Lett.*, *19*, 1731–1734, doi:10.1029/92GL01993.
Lühr, H., M. Rother, K. Kohler, P. Ritter, and L. Grunwaldt (2004), Thermospheric up-welling in the cusp region: Evidence from CHAMP observations, *Geophys. Res. Lett.*, *31*, L06805, doi:10.1029/2003GL019314.
Ma, T.-Z., and R. W. Schunk (1997), Effect of Sun-aligned arcs on the polar thermosphere, *J. Geophys. Res.*, *102*, 9729–9735, doi:10.1029/97JA00294.
McEwen, D. J., and D. P. Harris (1996), Occurrence patterns of *F* region layer patches over the north magnetic pole, *Radio Sci.*, *31*, 619–628, doi:10.1029/96RS00312.
McWilliams, K. A., T. K. Yeoman, and G. Provan (2000), A statistical survey of dayside pulsed ionospheric flows as seen by the CUTLASS Finland HF radar, *Ann. Geophys.*, *18*, 445–453, doi:10.1007/s00585-000-0445-8.
Milan, S. E., M. Lester, S. W. H. Cowley, and M. Brittnacher (2000), Convection and auroral response to a southward turning of the IMF: Polar UVI, CUTLASS, and IMAGE signatures of transient magnetic 410 flux transfer at the magnetopause, *J. Geophys. Res.*, *105*(A7), 15,741–15,755, doi:10.1029/2000JA900022.
Millward, C. H., R. J. Moffett, H. F. Balmforth, and A. S. Rodger (1999), Modeling the ionospheric effects of ion and electron precipitation in the cusp, *J. Geophys. Res.*, *104*, 24,603–24,612, doi:10.1029/1999JA900249.
Moen, J., H. C. Carlson, S. E. Milan, N. Shumilov, B. Lybekk, P. E. Sandholt, and M. Lester (2000), On the collocation between dayside auroral activity and coherent HF radar backscatter, *Ann. Geophys.*, *18*, 1531–1549, doi:10.1007/s00585-001-1531-2.
Moen, J., K. Oksavik, and H. C. Carlson (2004), On the relationship between ion upflow events and cusp auroral transients, *Geophys. Res. Lett.*, *31*, L11808, doi:10.1029/2004GL020129.
Moen, J., H. C. Carlson, K. Oksavik, C. P. Nielsen, S. E. Pryse, H. R. Middleton, I. W. McCrea, and P. Gallop (2006), EISCAT observations of plasma patches at sub-auroral cusp latitudes, *Ann. Geophys.*, *24*(9), 2363–2374, doi:10.5194/angeo-24-2363-2006.
Moen, J., N. Gulbrandsen, D. A. Lorentzen, and H. C. Carlson (2007), On the MLT distribution of F region polar cap patches at night, *Geophys. Res. Lett.*, *34*, L14113, doi:10.1029/2007GL029632.
Moen, J., Y. Rinne, H. C. Carlson, K. Oksavik, R. Fujii, and H. Opgenoorth (2008), On the relationship between narrow Birkeland current sheets and reversed flow channels in the winter cusp/cleft ionosphere, *J. Geophys. Res.*, *113*, A09220, doi:10.1029/2008JA013061.
Neudegg, D. A., et al. (2000), A survey of magnetopause FTEs and associated flow bursts in the polar ionosphere, *Ann. Geophys.*, *18*, 416–435, doi:10.1007/s00585-000-0416-0.
Oksavik, K., J. Moen, H. C. Carlson, R. A. Greenwald, S. E. Milan, M. Lester, W. F. Denig, and R. J. Barnes (2005), Multi-instrument mapping of the small-scale flow dynamics related to a cusp auroral transient, *Ann. Geophys.*, *23*, 2657–2670, doi:10.5194/angeo-23-2657-2005.
Oksavik, K., J. M. Ruohoniemi, R. A. Greenwald, J. B. H. Baker, J. Moen, H. C. Carlson, T. K. Yeoman, and M. Lester (2006), Observations of isolated polar cap patches by the European Incoherent Scatter (EISCAT) Svalbard and Super Dual Auroral Radar Network (SuperDARN) Finland radars, *J. Geophys. Res.*, *111*, A05310, doi:10.1029/2005JA011400.
Oksavik, K., V. L. Barth, J. Moen, and M. Lester (2010), On the entry and transit of high density plasma across the polar cap, *J. Geophys. Res.*, *115*, A12308, doi:10.1029/2010JA015817.
Oksavik, K., J. Moen, E. H. Rekaa, H. C. Carlson, and M. Lester (2011), Reversed flow events in the cusp ionosphere detected by SuperDARN HF radars, *J. Geophys. Res.*, *116*, A12303, doi:10.1029/2011JA016788.
Pinnock, M., A. S. Rodger, J. R. Dudeney, K. B. Baker, P. T. Newell, R. A. Greenwald, and M. E. Greenspan (1993), Observations of an Enhanced convection channel in the cusp ionosphere, *J. Geophys. Res.*, *98*(A3), 3767–3776, doi:10.1029/92JA01382.
Pinnock, M., A. S. Rodger, J. R. Dudeney, F. Rich, and K. B. Baker (1995), High spatial and temporal resolution observations of the ionospheric cusp, *Ann. Geophys.*, *13*, 919–925, doi:10.1007/s00585-995-0919-9.
Prikryl, P., J. W. MacDougal, I. F. Grant, D. P. Steel, G. J. Sofko, and R. A. Greenwald (1999), Observations of polar patches generated by solar wind Alfven wave coupling to the Dayside magnetosphere, *Ann. Geophys.*, *17*, 463–489, doi:10.1007/s00585-999-0463-0.
Rinne, Y., J. Moen, K. Oksavik, and H. C. Carlson (2007), Reversed flow events in the winter cusp ionosphere observed by the European Incoherent Scatter (EISCAT) Svalbard radar, *J. Geophys. Res.*, *112*, A10313, doi:10.1029/2007JA012366.
Rodger, A. S., M. Pinnock, J. R. Dudeney, K. B. Baker, and R. A. Greenwald (1994), A new mechanism for polar patch formation, *J. Geophys. Res.*, *99*(A4), 6425–6436, doi:10.1029/93JA01501.
Rodger, A. S., S. B. Mende, T. J. Rosenberg, and K. B. Baker (1995), Simultaneous optical and HF radar observations of the ionospheric cusp, *Geophys. Res. Lett.*, *22*(15), 2045–2048, doi:10.1029/95GL01797.
Sandholt, P. E., H. C. Carlson, and A. Egeland (2002), *Dayside and Polar Cap Aurora*, Kluwer, Dordrecht, Netherlands.
Schunk, R. W., and J. J. Sojka (1996), Ionosphere-thermosphere space weather issues, *J. Atmos. Terr. Phys.*, *58*, 1527–1574, doi:10.1016/0021-9169(96)00029-3.
Smith, M. F., and M. Lockwood (1996), Earth's magnetospheric cusps, *Rev. Geophys.*, *34*, 233–260, doi:10.1029/96RG00893.
Sojka, J. J., M. D. Bowline, R. W. Schunk, D. T. Decker, C. E. Valladares, R. Sheehan, D. N. Anderson, and R. A. Heelis (1993), Modeling polar cap *F*-region patches using time varying convection, *Geophys. Res. Lett.*, *20*(17), 1783–1786, doi:10.1029/93GL01347.
Sojka, J. J., M. D. Bowline, and R. W. Schunk (1994), Patches in the polar ionosphere: UT and seasonal dependence, *J. Geophys. Res.*, *99*(A8), 14,959–14,970, doi:10.1029/93JA03327.
Thayer, J. P., and J. Semeter (2004), The convergence of magnetospheric energy flux in the polar atmosphere, *J. Atmos. Sol. Terr. Phys.*, *66*, 807–824, doi:10.1016/j.jastp.2004.01.035.
Tsunoda, R. T. (1988), High-latitude *F* region irregularities: A review and synthesis, *Rev. Geophys.*, *26*(4), 719–760, doi:10.1029/RG026i004p00719.
Valladares, C. E., and H. C. Carlson (1991), The electrodynamic, thermal, and energetic character of intense Sun-aligned arcs in the polar cap, *J. Geophys. Res.*, *96*, 1379–1400, doi:10.1029/90JA01765.
Valladares, C. E., H. C. Carlson, and K. Fukui (1994), Interplanetary magnetic field dependency of stable Sun-aligned arcs, *J. Geophys. Res.*, *99*, 6247–6272, doi:10.1029/93JA03255.

Valladares, C. E., D. T. Decker, R. Sheehan, D. N. Anderson, T. Bullett, and B. W. Reinisch (1998), Formation of polar cap patches associated with north-to-south transitions of the interplanetary magnetic field, *J. Geophys. Res.*, *103*(A7), 14,657–14,670, doi:10.1029/97JA03682.

Valladares, C. E., J. Moen, P. E. Sandholt, W. F. Denig, and O. Troshichev (2002), Simultaneous observations of dayside aurora from Heiss Island and Ny Ålesund, *Geophys. Res. Lett.*, *29*(24), 2202, doi:10.1029/2002GL016001.

Weber, E. J., and J. Buchau (1981), Polar cap F-455 layer auroras, *Geophys. Res. Lett.*, *8*, 125–128, doi:10.1029/GL008i001p00125.

Weber, E. J., J. J. Buchau, J. G. Moore, J. R. Sharber, R. C. Livingston, J. D. Winningham, and B. W. Reinish (1984), *F* layer ionization patches in the polar cap, *J. Geophys. Res.*, *89*(A3), 1683–1694, doi:10.1029/JA089iA03p01683.

Weber, E. J., J. A. Klobuchar, J. Buchau, H. C. Carlson, R. C. Livingston, O. de la Beaujardiere, M. McCready, J. G. Moore, and G. J. Bishop (1986), Polar cap *F* layer patches: Structure and dynamics, *J. Geophys. Res.*, *91*(A11), 12,121–12,129, doi:10.1029/JA091iA11p12121.

Zhu, L., R. W. Schunk, and J. J. Sojka (1997), Polar-cap arcs: A review, *J. Atmos. Sol. Terr. Phys.*, *59*, 1087–1126, doi:10.1016/S1364-6826(96)00113-7.